Unfolding of plasmon-polariton modes in one-dimensional layered systems containing anisotropic left-handed materials

A. Bruno-Alfonso,[1] E. Reyes-Gómez,[2] S. B. Cavalcanti,[3] and L. E. Oliveira[4]
[1]*Departamento de Matemática, Faculdade de Ciências, UNESP, 17033-360 Bauru, São Paulo, Brazil*
[2]*Instituto de Física, Universidad de Antioquia, AA 1226 Medellín, Antioquia, Colombia*
[3]*Instituto de Física, UFAL, Cidade Universitária, 57072-970 Maceió, Alagoas, Brazil*
[4]*Instituto de Física, UNICAMP, 13083-859 Campinas, São Paulo, Brazil*
(Received 15 March 2011; revised manuscript received 15 June 2011; published 6 September 2011)

The propagation of electromagnetic waves through a 1-dimensional layered system containing alternate layers of air and a uniaxial, anisotropic, left-handed material is investigated. The optical axis of this material is along the stacking direction and the components of the electric permittivity and magnetic permeability tensors that characterize the metamaterial are described by Drude-type responses. Different plasmon frequencies are considered for directions parallel and perpendicular to the optical axis. As in the isotropic case, plasmon polariton modes are found in the neighborhood of the plasmon frequency corresponding to the optical axis. Moreover, it is shown that, depending on the relation between the two plasmon frequencies of the metamaterial, anisotropy leads to the unfolding of an infinite number of nearly dispersionless plasmon-polariton bands either above or below the parallel plasmon frequency.

DOI: 10.1103/PhysRevB.84.113101 PACS number(s): 42.25.Bs, 42.70.Qs, 78.20.Bh

In the last two decades, a number of both experimental and theoretical studies have been devoted to understanding the properties of wave propagation in photonic crystals, which are artificial periodic arrays of materials with different refractive indices. As a result, interesting properties of light confinement and manipulation of electromagnetic waves in these matter structures have attracted a great deal of interest, due to potential applications to optical devices such as optical filters,[1–3] optical switches,[4] optical logic devices,[5] and optical buffers.[6,7] By producing sophisticated microstructured materials, one may obtain artificial media with unusual features, such as simultaneous negative dielectric permittivity ε and magnetic permeability μ. These so-called metamaterials may be engineered to enhance the role played by the magnetic component of the electromagnetic field, giving rise to novel regimes of light-matter interaction. An interface between a material with positive permittivity and another with negative permittivity may support *surface* plasmon polaritons,[8] a result of the coupling of the incident electromagnetic radiation with the charge density of the material. Recent work on 1-dimensional (1D) photonic heterostructures formed by alternating a right-handed material (RHM), such as air, with an ideal isotropic left-handed material (LHM) has evidenced the existence of a zero-$\langle n\rangle$ (null average of the refractive index) band gap[9–15] that is insensitive to lattice parameter changes (in contrast to the behavior exhibited by Bragg gaps), and exhibited *bulk* plasmon polariton modes, whether the stacking arrangement is periodic, quasiperiodic, or even disordered.[16–23] However, in practice, an isotropic LHM is still a great challenge for researchers, as the available LHM structures are intrinsically anisotropic. The reflection from a 1D photonic heterostructure containing an anisotropic LHM has been investigated by Wang and Gao.[24] Moreover, Sun *et al.*[25] have reported on a two-dimensional (2D) complete photonic band gap in this type of structure. Recently, the unfolding of nearly dispersionless modes has been reported[26] in a 2D, highly anisotropic arrangement of hexagonal shell rods of *n*-doped GaAs embedded in air. Furthermore, light-matter interaction in quasiperiodic RHM-LHM stacks has also resulted in the unfolding of plasmon-polariton modes in the neighborhood of the plasmon frequency, in contrast with the periodic case.[20–22]

In this report we extend the investigations of RHM-LHM photonic 1D superlattices by considering the substitution of the dispersive isotropic LHM component by an anisotropic one[27–29] in order to answer the question of whether the physical behavior of the anisotropic metamaterial changes as compared to the isotropic ones. In the following development we show that anisotropy leads to the appearance of essentially dispersionless plasmon-polariton bands and we provide an approximate analytical expression for such bands.

Here we consider a RHM-LHM photonic 1D superlattice consisting of alternate layers of materials A and B, of widths d_A and d_B, respectively, stacked along the z axis. Moreover, the origin of this axis separates a layer B (to the left) from a layer A (to the right) and the length of the unit cell is $d = d_A + d_B$. Material A is a nondispersive isotropic RHM, with scalar dielectric permittivity ε_A and magnetic permeability μ_A. For simplicity, we assume that B is a uniaxial metamaterial with the optical axis along the stacking direction. Accordingly, $\boldsymbol{\varepsilon}_B$ and $\boldsymbol{\mu}_B$ are diagonal tensors with $\varepsilon_{B,xx} = \varepsilon_{B,yy} = \varepsilon_{B,\perp}$, $\varepsilon_{B,zz} = \varepsilon_{B,\parallel}$, $\mu_{B,xx} = \mu_{B,yy} = \mu_{B,\perp}$, and $\mu_{B,zz} = \mu_{B,\parallel}$. Hence, the relations between the intensity and induction vectors of the electromagnetic field are described by the position-dependent tensors $\boldsymbol{\varepsilon}(z)$ and $\boldsymbol{\mu}(z)$, namely $\mathbf{D} = \varepsilon_0\,\boldsymbol{\varepsilon}(z)\cdot\mathbf{E}$ and $\mathbf{B} = \mu_0\,\boldsymbol{\mu}(z)\cdot\mathbf{H}$, where ε_0 and μ_0 are the permittivity and permeability values of the vacuum, respectively. Moreover, due to the periodicity of the 1D photonic superlattice, equations $\boldsymbol{\varepsilon}(z+d) = \boldsymbol{\varepsilon}(z)$ and $\boldsymbol{\mu}(z+d) = \boldsymbol{\mu}(z)$ hold.

In order to investigate the propagation of monochromatic electromagnetic waves, one may write $\mathbf{E}(\mathbf{r},t) = e^{-i\omega t}\mathbf{E}(\mathbf{r})$ and $\mathbf{H}(\mathbf{r},t) = e^{-i\omega t}\mathbf{H}(\mathbf{r})$. In this way, the spatial parts of the electromagnetic field satisfy

$$\nabla\times\mathbf{E} = i\omega\mu_0\,\boldsymbol{\mu}(z)\cdot\mathbf{H} \tag{1}$$

and

$$\nabla \times \mathbf{H} = -i\omega\varepsilon_0\, \boldsymbol{\varepsilon}(z)\cdot \mathbf{E}. \tag{2}$$

Because of the periodicity of $\boldsymbol{\varepsilon}(z)$ and $\boldsymbol{\mu}(z)$, the intensities of the electromagnetic field satisfy the Bloch condition, i.e., $\mathbf{E}(\mathbf{r}+\mathbf{R}) = e^{i\mathbf{k}\cdot\mathbf{R}}\mathbf{E}(\mathbf{r})$ and $\mathbf{H}(\mathbf{r}+\mathbf{R}) = e^{i\mathbf{k}\cdot\mathbf{R}}\mathbf{H}(\mathbf{r})$ for every translation vector of the crystal lattice. Moreover, the wave is assumed to propagate parallel to the xz plane; i.e., we take $\mathbf{k} = q\mathbf{e}_x + k\mathbf{e}_z$.

For the transversal magnetic (TM) polarization, we take $\mathbf{H}(\mathbf{r}) = H_0\, h(z)\exp(iqx)\,\mathbf{e}_y$, where $h(z)$ is a dimensionless function. The Bloch condition reads $h(z+d) = e^{ikd}\, h(z)$. According to Eq. (2), the electric field is $\mathbf{E}(\mathbf{r}) = \exp(iqx)[E_x(z)\,\mathbf{e}_x + E_z(z)\,\mathbf{e}_z]$, where $E_x(z) = -i\, H_0\, f(z)/(c\,\varepsilon_0)$ and $E_z(z) = -q\, H_0\, h(z)/[\omega\,\varepsilon_0\,\varepsilon_{zz}(z)]$, with $f(z) = c\,h'(z)/[\omega\ \varepsilon_{xx}(z)]$. This dimensionless function also satisfies the Bloch condition; i.e., $f(z+d) = e^{ikd}\, f(z)$ applies. Moreover, Eq. (1) leads to

$$-f'(z) = \left[\frac{\omega\,\mu_{yy}(z)}{c} - \frac{c\,q^2}{\omega\,\varepsilon_{zz}(z)}\right] h(z). \tag{3}$$

Therefore, $h(z)$ satisfies the following equation:

$$-\frac{d}{dz}\frac{1}{\varepsilon_{xx}(z)}\frac{d}{dz}h(z) = \left[\frac{\omega^2\mu_{yy}(z)}{c^2} - \frac{q^2}{\varepsilon_{zz}(z)}\right] h(z). \tag{4}$$

Also, for each pair (z_0,z), there is a transfer matrix, $\mathbf{T}(\omega,z,z_0)$, such that

$$\begin{bmatrix} h(z) \\ f(z) \end{bmatrix} = \mathbf{T}(\omega,z,z_0)\begin{bmatrix} h(z_0) \\ f(z_0) \end{bmatrix}. \tag{5}$$

For the investigated structure, the transfer matrix between z_0 and $z > z_0$ is given by $\mathbf{T}(\omega,z,z_0) = \mathbf{T}_l \cdot \mathbf{T}_{l-1} \cdot \ldots \cdot \mathbf{T}_2 \cdot \mathbf{T}_1$, where $\mathbf{T}_i$ transfers across the ith among the l homogeneous regions between z_0 and z ($i = 1,\ldots,l$ increases from z_0 to z). In particular, the transfer matrix between points z and $z+\Delta z$ within a region of permittivities $\varepsilon_{L,\perp}$ and $\varepsilon_{L,\parallel}$ and permeabilities $\mu_{L,\perp}$ and $\mu_{L,\parallel}$, where L may be either A or B, is written as

$$\mathbf{T}_L(\omega,\Delta z) = \begin{bmatrix} \cos(Q_L\Delta z) & \frac{\omega\varepsilon_{L,\perp}}{cQ_L}\sin(Q_L\Delta z) \\ -\frac{cQ_L}{\omega\varepsilon_{L,\perp}}\sin(Q_L\Delta z) & \cos(Q_L\Delta z) \end{bmatrix}, \tag{6}$$

with $Q_L = \sqrt{\frac{\omega^2\varepsilon_{L,\perp}\mu_{L,\perp}}{c^2} - q^2\frac{\varepsilon_{L,\perp}}{\varepsilon_{L,\parallel}}}$.

To obtain the relation between the wave frequency and the wave vector, it is useful to consider the matrix

$$\mathbf{M}(\omega) = \mathbf{T}(\omega,d,0) = \mathbf{T}_B(\omega,d_B)\cdot\mathbf{T}_A(\omega,d_A), \tag{7}$$

which connects $h(0)$ and $f(0)$ with $h(d)$ and $f(d)$. Hence, by taking into account the Bloch condition, we get[30]

$$\cos(kd) = m(\omega), \tag{8}$$

where

$$m(\omega) = \cos(Q_A\,d_A)\cos(Q_B\,d_B) - \frac{1}{2}\left(\frac{\varepsilon_A\,Q_B}{\varepsilon_{B,\perp}\,Q_A} + \frac{\varepsilon_{B,\perp}\,Q_A}{\varepsilon_A\,Q_B}\right)\sin(Q_A\,d_A)\sin(Q_B\,d_B) \tag{9}$$

is the semitrace of $\mathbf{M}(\omega)$. For each $j = 1,2,\ldots$ Eq. (8) implicitly defines the frequency bands $\omega_j(k)$.

In this paper, we limit the investigation to the electromagnetic modes above the light line of material A, such that $\omega > q\,c/n_A$. In this case, the components of the wave vector along the x and z axes take real values q and Q_A, respectively. Thus, the allowed frequencies may be calculated in terms of the angle θ between the z axis and the wave vector within material A. It is worth noting that if a finite RHM-LHM 1D layered sample is embedded in optical medium A, then θ is the incidence angle of the electromagnetic waves. This angle satisfies $q = \frac{\omega n_A}{c}\sin(\theta)$, $Q_A = \frac{\omega n_A}{c}\cos(\theta)$, and $Q_B = \frac{\omega}{c}\sqrt{\varepsilon_{B,\perp}\mu_{B,\perp} - n_A^2\sin^2(\theta)\frac{\varepsilon_{B,\perp}}{\varepsilon_{B,\parallel}}}$.

For the transversal electric (TE) polarization, we take $\mathbf{E}(\mathbf{r}) = E_0\, f(z)\exp(iqx)\,\mathbf{e}_y$, where $f(z)$ is a dimensionless function that satisfies the Bloch condition. According to Eq. (2), the magnetic field is $\mathbf{H}(\mathbf{r}) = \exp(iqx)[H_x(z)\,\mathbf{e}_x + H_z(z)\,\mathbf{e}_z]$, where $H_x(z) = i\,E_0\,h(z)/(c\,\mu_0)$ and $H_z(z) = q\,E_0\,f(z)/[\omega\,\mu_0\,\mu_{zz}(z)]$, with $h(z) = c\,f'(z)/[\omega\,\mu_{xx}(z)]$. Again, $h(z)$ is dimensionless and satisfies the Bloch condition. Furthermore, Eq. (2) leads to

$$-h'(z) = \left[\frac{\omega\varepsilon_{yy}(z)}{c} - \frac{c\,q^2}{\omega\,\mu_{zz}(z)}\right] f(z). \tag{10}$$

Therefore, $f(z)$ satisfies the following equation

$$-\frac{d}{dz}\frac{1}{\mu_{xx}(z)}\frac{d}{dz}f(z) = \left[\frac{\omega^2\varepsilon_{yy}(z)}{c^2} - \frac{q^2}{\mu_{zz}(z)}\right] f(z). \tag{11}$$

Moreover, the transfer matrix is defined by

$$\begin{bmatrix} f(z) \\ h(z) \end{bmatrix} = \mathbf{T}(\omega,z,z_0)\begin{bmatrix} f(z_0) \\ h(z_0) \end{bmatrix}, \tag{12}$$

and the transfer between z and $z+\Delta z$ within layer L is given by

$$\mathbf{T}_L(\omega,\Delta z) = \begin{pmatrix} \cos(Q_L\Delta z) & \frac{\omega\mu_{L,\perp}}{cQ_L}\sin(Q_L\Delta z) \\ -\frac{cQ_L}{\omega\mu_{L,\perp}}\sin(Q_L\Delta z) & \cos(Q_L\Delta z) \end{pmatrix}, \tag{13}$$

with $Q_L = \sqrt{\frac{\omega^2\varepsilon_{L,\perp}\mu_{L,\perp}}{c^2} - q^2\frac{\mu_{L,\perp}}{\mu_{L,\parallel}}}$ (see Sun *et al.*[25]) Moreover, the semitrace of $\mathbf{M}(\omega) = \mathbf{T}(\omega,d,0)$ is

$$m(\omega) = \cos(Q_A\,d_A)\cos(Q_B\,d_B) - \frac{1}{2}\left(\frac{\mu_A\,Q_B}{\mu_{B,\perp}\,Q_A} + \frac{\mu_{B,\perp}\,Q_A}{\mu_A\,Q_B}\right)\sin(Q_A\,d_A)\sin(Q_B\,d_B). \tag{14}$$

In this case, the component of the wave vector along the z-axis direction in the metamaterial is $Q_B = \frac{\omega}{c}\sqrt{\varepsilon_{B,\perp}\mu_{B,\perp} - n_A^2\sin^2(\theta)\frac{\mu_{B,\perp}}{\mu_{B,\parallel}}}$.

We present numerical results for the TM modes in a RHM-LHM photonic 1D superlattice whose unit cell consists of an air layer denoted by A ($\varepsilon_A = \mu_A = 1$) and an anisotropic left-handed material denoted by B. The dielectric permittivity $\boldsymbol{\varepsilon}_B$ and magnetic permeability $\boldsymbol{\mu}_B$ are given by $\varepsilon_{B,\alpha} = \varepsilon_{\infty,\alpha}(1 - \omega_{e,\alpha}^2/\omega^2)$ and $\mu_{B,\alpha} = \mu_{\infty,\alpha}(1 - \omega_{m,\alpha}^2/\omega^2)$, where $\alpha = \perp$ or $\parallel$. Moreover, in what follows, we use frequency values $\nu = \omega/(2\pi)$, $\nu_{e,\alpha} = \omega_{e,\alpha}/(2\pi)$ and $\nu_{m,\alpha} = \omega_{m,\alpha}/(2\pi)$.

The case of isotropic layer B has already been studied by Reyes-Gómez *et al.*[20] For comparison purposes, we calculate

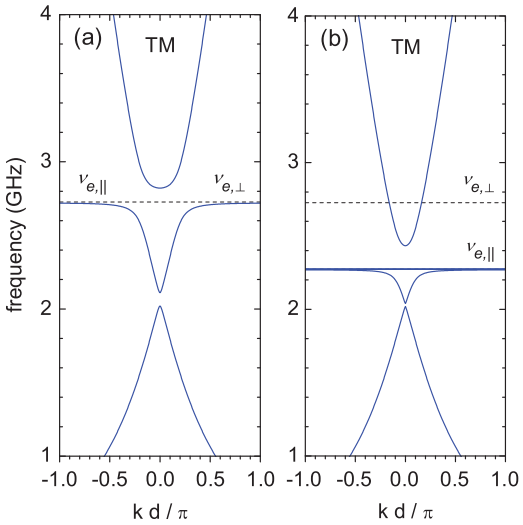

FIG. 1. (Color online) Frequency of TM modes as a function of wave vector k, for $\theta = \pi/12$ in a RHM-LHM photonic 1D superlattice with $d_A = d_B = 12$ mm and $\nu_{m,\perp} = \nu_{m,\parallel} = 3$ GHz. (a) Isotropic metamaterial with $\nu_{e,\parallel} = \nu_{e,\perp} = 2.7273$ GHz. (b) Anisotropic metamaterial with $\nu_{e,\perp} = 2.7273$ GHz and $\nu_{e,\parallel} = 2.2727$ GHz.

the TM modes for $\theta = \pi/12$ in a RHM-LHM photonic 1D superlattice with $d_A = d_B = 12$ mm, $\varepsilon_{\infty,\perp} = \varepsilon_{\infty,\parallel} = 1.21$, $\mu_{\infty,\perp} = \mu_{\infty,\parallel} = 1.00$, $\nu_{e,\perp} = \nu_{e,\parallel} = 2.7273$ GHz, and $\nu_{m,\perp} = \nu_{m,\parallel} = 3$ GHz, as in Ref. 20 with results displayed in Fig. 1(a). This is in agreement with the discussion in Ref. 20 of light-matter interaction leading to coupled plasmon-polariton modes. To probe the effects of anisotropy on the TM modes, we perform the calculations for the same set of parameters as above, except for $\nu_{e,\parallel} = \frac{5}{6}\nu_{e,\perp} = 2.2727$ GHz. One may note that the two lowest-frequency bands shown in panels 1(a) and 1(b) are separated by the $\langle n \rangle = 0$ gap, near 2 GHz [as this gap is rather small, it is not easily seen in 1(b)]. The width of this gap is affected by anisotropy, but the gap survives in all cases.

As shown in Fig. 1(b), the essentially dispersionless plasmon-polariton bands occur near the plasmon frequency $\nu_{e,\parallel}$. Solid lines in Fig. 2 display the four highest among the nearly flat plasmon-polariton bands around $\nu_{e,\parallel}$. In this frequency range, it is straightforward to show that

$$Q_B \approx \frac{\pi}{d_B}\sqrt{\frac{\beta}{\frac{\nu}{\nu_{e,\parallel}} - 1}}, \tag{15}$$

with $\beta = 2\,d_B^2\,n_A^2\sin^2(\theta)\,(\nu_{e,\perp}^2 - \nu_{e,\parallel}^2)\,\varepsilon_{\infty,\perp}/(c^2\,\varepsilon_{\infty,\parallel})$. Then, the second term of $m(\omega)$ in Eq. (9) will diverge to infinity unless $Q_A d_A \approx n\pi$ or $Q_B d_B \approx n\pi$, for a positive integer n. However, the first of these two conditions applies for frequencies far away from $\nu_{e,\parallel}$. In fact, it leads to $\nu \approx n\,c/[2n_A\,d_A\,\cos(\theta)] \geqslant n\,c/(2n_A\,d_A) > 4.1$ GHz. The second condition, $Q_B d_B \approx n\pi$, since we are dealing with the case $\beta \approx 0.0005 > 0$, applies only for frequencies above $\nu_{e,\parallel}$. To obtain the approximate shape of the corresponding bands, we write $Q_B d_B = [n + \delta_n(k)]\pi$. Then, we take $\nu \approx \nu_{e,\parallel}$, make a

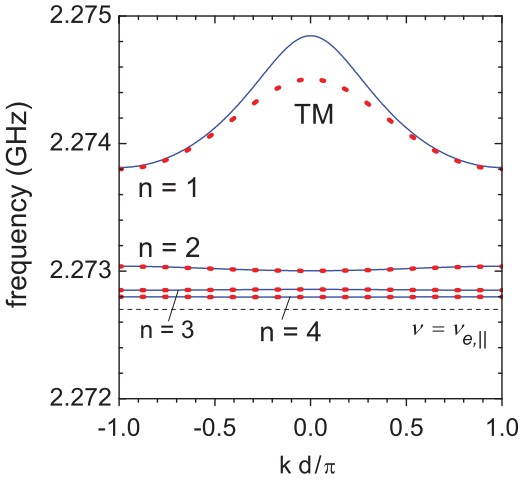

FIG. 2. (Color online) Solid lines are the four highest nearly dispersionless plasmon-polariton bands just above the frequency $\nu_{e,\parallel}$ in Fig. 1(b). Dots are for $n = 1, \ldots, 4$ in Eq. (17).

first-order Taylor expansion of $m(\omega)$ in $\delta_n(k)$, and substitute into Eq. (8) to obtain

$$\delta_n(k) = \frac{2d_B\varepsilon_{\infty,\perp}\left(1 - \frac{\nu_{e,\perp}^2}{\nu_{e,\parallel}^2}\right)\,[\cos(\phi) - (-1)^n\cos(kd)]}{n\pi^2 d_A\varepsilon_A\,\sin(\phi)/\phi}, \tag{16}$$

with $\phi = 2\pi\,\nu_{e,\parallel}n_A d_A\cos(\theta)/c$. Moreover, following Eq. (15), the investigated bands are essentially given by

$$\nu \approx \nu_{e,\parallel}\left\{1 + \frac{\beta}{[n + \delta_n(k)]^2}\right\}. \tag{17}$$

To assess this approximation, the results for $n = 1,2,3$, and 4 are displayed as dots in Fig. 2. We observe that Eq. (17) is in good agreement with the exact results. Moreover, the agreement is better for larger values of n. In fact, from Eq. (16), the maximum value of $|\delta_n(k)|$ decreases as n increases, thus making our approximations more reliable. This demonstrates the existence of an infinite series of plasmon-polariton bands in the small frequency range under consideration.

Now the diagonal permittivity along the z axis is taken as $\nu_{e,\parallel} = \frac{7}{6}\nu_{e,\perp} = 3.1818$ GHz, while all other parameters remain the same. Figure 3(a) shows that the nondispersive parts of the plasmon-polariton bands occur near the plasmon frequency $\nu_{e,\parallel}$. Moreover, since $\beta \approx -0.0006 < 0$, the infinite series of nearly flat plasmon-polariton bands is just below $\nu_{e,\parallel}$ [see Eq. (15)]. This is illustrated in Fig. 3(b), where dots correspond to results of approximation in Eq. (17) for $n = 1, \ldots, 4$.

It should be remarked that the width of the frequency range containing the infinite series of nearly flat bands is of the order of $|\beta|\,\nu_{e,\parallel} \propto d_B^2\,n_A^2\sin^2(\theta)\,|\nu_{e,\perp} - \nu_{e,\parallel}|$. Therefore, this width tends to zero when either $\theta \to 0$ or $\nu_{e,\parallel} \to \nu_{e,\perp}$, and the series of nearly dispersionless bands folds into an infinitely degenerate frequency at $\nu_{e,\parallel}$. Conversely, when the metamaterial is anisotropic, oblique incidence produces the unfolding of the degenerate plasmon frequency into the investigated series of bands. Moreover, this unfolding should be more noticeable for larger values of θ, d_B, and n_A.

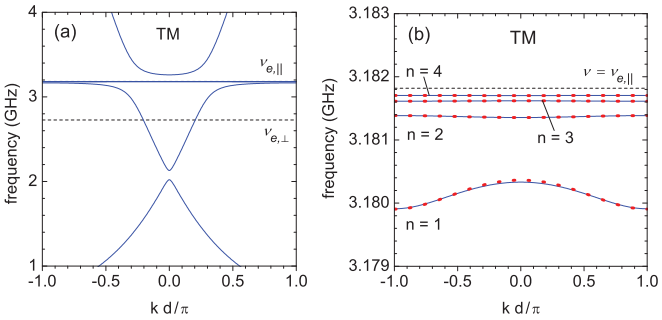

FIG. 3. (Color online) (a) Frequency of TM modes as a function of wave vector k, for $\theta = \pi/12$, in a RHM-LHM photonic 1D superlattice with $d_A = d_B = 12$ mm. Metamaterial B is anisotropic with $\nu_{e,\perp} = 2.7273$ GHz, $\nu_{e,\parallel} = 3.1818$ GHz, and $\nu_{m,\perp} = \nu_{m,\parallel} = 3$ GHz. (b) Solid lines are the four lowest plasmon-polariton bands just below the frequency $\nu_{e,\parallel}$ in panel (a). Dots are for results of Eq. (17) when $n = 1, \ldots, 4$.

It is important to stress that a fundamental limitation of metamaterials is their absorptive nature, which would certainly compromise, in real systems, the resolution of the sub-bands found here. Nevertheless, besides the fact that the theoretical prediction of these nearly dispersionless plasmon-polariton modes should be relevant for a comprehensive understanding of metamaterial structures, researchers worldwide are putting efforts into fabrication techniques that compensate the losses that dampen the plasmon polaritons in metamaterial heterostructures. Thus, the combination of metamaterials with electrically and optically pumped gain media, as well as emerging graphene technology are expected to lead to remarkable progress in metamaterial engineering, providing low-loss materials suitable for use in optical devices and in the electronic industry.[31–35]

Summing up, we have dealt theoretically with TM and TE modes of a RHM-LHM photonic 1D superlattice with a unit cell consisting of a layer of air and a layer of an anisotropic LHM. Numerical results are shown here for TM modes only. However, because of the equivalence between differential equations (4) and (11), similar results should be obtained for TE modes, provided the corresponding parameters of the dielectric-permittivity and magnetic-permeability tensors are interchanged. For TM (TE) configuration, the essentially dispersionless electric (magnetic) plasmon polariton bands occur near the frequency where the diagonal dielectric permittivity (magnetic permeability) along the stacking direction is zero, hence the bulk character of the plasmon mode. When this frequency is less (greater) than the plasmon frequency in the perpendicular direction, an infinite series of dispersionless bands is found just above (below) it. Simple analytic expressions to estimate the shapes of those bands have been given and analyzed. In comparison with the isotropic RHM-LHM photonic 1D superlattice, we find that anisotropy leads to the unfolding of essentially dispersionless plasmon-polariton bands in the same fashion as in the case of the 2D anisotropic GaAs photonic structure of dispersive rods embedded in air. We do hope that the results obtained here might help in the understanding of the physical reasons behind the appearance of dispersionless bands in 2D photonic structures.

We thank the Colombian agency CODI at the University of Antioquia and Brazilian agencies CNPq and FAPESP for partial financial support. The first three authors also acknowledge the warm hospitality of the IFGW-Unicamp, where part of this work was done.

[1] C. Zheng, H. Tian, C. Li, and Y. Li, Proc. SPIE **6781**, 678117 (2007).
[2] Y. Kanamori, N. Matsuyama, and K. Hane, IEEE Photonics Technol. Lett. **20**, 1136 (2008).
[3] H. Nemec, L. Duvillaret, and F. Garet, J. Appl. Phys. **96**, 4072 (2004).
[4] V. Ya. Zyryanov, V. A. Gunyakov, S. A. Myslivets, V. G. Arkhipkin, and V. F. Shabanov, Mol. Cryst. Liq. Cryst. **488**, 118 (2008).
[5] P. Andalib and N. Granpayeh, J. Opt. Soc. Am. B **26**, 10 (2009).
[6] T. Baba, Nat. Photonics **2**, 465 (2008).
[7] A. Di Falco, L. O'Faolain, and T. F. Krauss, Appl. Phys. Lett. **92**, 083501 (2008).
[8] L. D. Landau, E. M. Lifshitz, and L.P. Pitaevskii, *Electrodynamics of Continuous Media*, 2nd ed., Course of Theoretical Physics Vol. 8 (Reed Educational and Professional Publishing, Oxford, UK, 1984).
[9] J. Li, L. Zhou, C. T. Chan, and P. Sheng, Phys. Rev. Lett. **90**, 083901 (2003).
[10] H. Jiang, H. Chen, H. Li, Y. Zhang, and S. Zhu, Appl. Phys. Lett. **83**, 5386 (2003).
[11] J. Li, D. Zhao, and Z. Liu, Phys. Lett. A **332**, 461 (2004).
[12] N. C. Panoiu, R. M. Osgood Jr., S. Zhang, and S. R. J. Brueck, J. Opt. Soc. Am. B **23**, 506 (2006).
[13] Y. Xiang, X. Dai, and S. Wen, J. Opt. Soc. Am. B **24**, 2033 (2007).
[14] S. Kocaman, R. Chatterjee, N. C. Panoiu, J. F. McMillan, M. B. Yu, R. M. Osgood, D. L. Kwong, and C. W. Wong, Phys. Rev. Lett. **102**, 203905 (2009).
[15] S. B. Cavalcanti, M. de Dios-Leyva, E. Reyes-Gómez, and L. E. Oliveira, Phys. Rev. E **75**, 026607 (2007).
[16] J. A. Monsoriu, R. A. Depine, M. L. Martínez-Ricci, and E. Silvestre, Opt. Express **14**, 12958 (2006).
[17] H. Daninthe, S. Foteinopoulou, and C. M. Soukoulis, Photo. Nano. Fund. Appl. **4**, 123 (2006).
[18] R. A. Depine, M. L. Martínez-Ricci, J. A. Monsoriu, E. Silvestre, and P. Andrés, Phys. Lett. A **364**, 352 (2007).
[19] S. K. Singh, J. P. Pandey, K. B. Thapa, and S. P. Ojha, Solid State Commun. **143**, 217 (2007).
[20] E. Reyes-Gómez, D. Mogilevtsev, S. B. Cavalcanti, C. A. A. de Carvalho, and L. E. Oliveira, Europhys. Lett. **88**, 24002 (2009).
[21] E. Reyes-Gómez, N. Raigoza, S. B. Cavalcanti, C. A. A. de Carvalho, and L. E. Oliveira, Phys. Rev. B **81**, 153101 (2010).
[22] D. Mogilevtsev, F. A. Pinheiro, R. R. dos Santos, S. B. Cavalcanti, and L. E. Oliveira, Phys. Rev. B **82**, 081105(R) (2010).
[23] C. A. A. de Carvalho, S. B. Cavalcanti, E. Reyes-Gómez, and L. E. Oliveira, Phys. Rev. B **83**, 081408(R) (2011).

[24]S. Wang and L. Gao, Eur. Phys. J. B **48**, 29 (2005).
[25]S. Sun, X. Huang, and L. Zhou, Phys. Rev. E **75**, 066602 (2007).
[26]C. A. Duque, N. Porras-Montenegro, S. B. Cavalcanti, and L. E. Oliveira, J. Appl. Phys. **105**, 034303 (2009).
[27]I. Abdulhalim, J. Opt. A: Pure Appl. Opt. **11**, 015002 (2009).
[28]M. Liscidini and J. E. Sipe, Phys. Rev. B **81**, 115335 (2010).
[29]X. Wang, P. Wang, J. Chen, Y. Lu, H. Ming, and Q. Zhan, Appl. Phys. Lett. **98**, 021113 (2011).
[30]M. C. Romano, D. R. Nacbar, and A. Bruno-Alfonso, J. Phys. B: At., Mol. Opt. Phys. **43**, 215403 (2010).
[31]A. Fang, T. Koschny, and C. M. Soukoulis, J. Opt. A: Pure Appl. Opt. **12**, 024013 (2010).
[32]N. I. Zheludev, Science **328**, 582 (2010).
[33]S. Xiao, V. P. Drachev, A. V. Kildishev, X. Ni, U. K. Chettiar, H.-K. Yuan, and V. M. Shalaev, Nature (London) **466**, 735 (2010).
[34]A. Boltasseva and H. A. Atwater, Science **331**, 290 (2011).
[35]N. I. Zheludev, Opt. Photon. News **22**, 31 (2011).